

HEFAT2010  
7<sup>th</sup> International Conference on Heat Transfer, Fluid Mechanics and Thermodynamics  
19-21 July 2010  
Antalya, Turkey

## EVALUATION OF HEAT TRANSFER RATES AND WALL TEMPERATURES IN A HYDROGEN-FUELLED SPARK IGNITION ENGINE

Demuyneck J.\*, De Paepe M., Huisseune H., Sierens R. and Verhelst S.

\*Author for correspondence

Department of Flow, Heat and Combustion Mechanics,

Ghent University - UGent,

Gent, 9000,

Belgium,

E-mail: joachim.demuyneck@ugent.be

### ABSTRACT

Hydrogen-fuelled internal combustion engines are a possible solution to make transportation more ecological. A thermodynamic model of the engine cycle enables a cheap and fast optimization of engine settings. NO<sub>x</sub> emission occurs at high loads and is a constraint for power and efficiency optimization. The thermodynamic model has to predict accurately the heat transfer in the engine because the NO<sub>x</sub> emission is influenced by the maximum gas temperature. The existing engine heat transfer models in the literature are developed for fossil fuels and they have been cited to be inaccurate for hydrogen. We have measured the heat transfer inside a spark ignited engine with a thermopile to investigate the heat transfer process of hydrogen and to find the differences with fossil fuels. This paper describes the effects of the compression ratio, ignition timing and mixture richness on the heat transfer process. A convection coefficient is introduced to separate the effect of the temperature difference between the gas and the wall from the influence of the gas movement and the combustion process. The paper shows that the convection coefficient gives more insight in the heat transfer process in a combustion engine despite its doubtful definition. The maximum in the heat flux corresponds with the maximum of the temperature difference between the gas and the wall. The initial increase in the heat flux is caused by the combustion flame passage. The maximum of the convection coefficient occurs at the moment that the initial rising slope in the heat flux ends.

### INTRODUCTION

Climate change and energy supply are high on the political agenda these days. We have to move away from the fossil fuel based energy supply of today. The transportation sector in particular is very dependent on fossil fuels. There are many alternatives but no silver bullet, so several promising possibilities are investigated at the Transportation Technology research group of Ghent University.

One of them is the hydrogen-fuelled combustion engine. Research has proven that the combustion properties of

hydrogen enable a high efficiency and a wide range of operational strategies [1]. Moreover, hydrogen engines have near-zero noxious and zero greenhouse gas emissions which makes them an attractive alternative for the current drive trains.

The initial research at Ghent University was focused on the experimental optimization of engine operation strategies for maximum power and efficiency, with ultra low nitric oxide emissions [2-4]. The focus shifted to numerical research with the development of a thermodynamic model of the engine cycle, the GUEST-code (Ghent University Engine Simulation Tool) [5, 6].

A thermodynamic model of the engine cycle enables a cheap and fast optimization of engine settings for operation on hydrogen. Several sub models are necessary to solve the conservation equations of energy and mass: a combustion, a turbulence and a heat transfer model among others. The last one is important to simulate accurately the emissions of oxides of nitrogen which are influenced by the maximum gas temperature. These emissions can occur in hydrogen internal combustion engines at high loads and they are an important constraint for power and efficiency optimization.

Several heat transfer models for internal combustion engines (ICE) exist in the literature, but they have been developed for fossil-fuelled engines and are cited to be inaccurate for hydrogen [7, 8].

We have measured heat transfer rates and wall temperatures in a hydrogen-fuelled spark ignited engine with a commercially available heat flux sensor [9]. The purpose of the research is to find the differences in the heat transfer caused by hydrogen and a fossil fuel. This paper describes a more profound investigation of those measurements to find the parameters which are influencing the heat transfer process in a combustion engine. It describes the effects of the compression ratio, ignition timing and mixture richness on the heat transfer.

## NOMENCLATURE

## Abbreviations

$^{\circ}CA$	degree crank angle
$NO_x$	oxides of nitrogen
ABDC	after bottom dead centre
ATDC	after top dead centre
BBDC	before bottom dead centre
BTDC	before top dead centre
CFR	Cooperative Fuel Research
EVC	exhaust valve closure
EVO	exhaust valve opening
HFM	heat flux microsensor
HFS	heat flux sensor
IGN	ignition timing
IVC	intake valve closure
IVO	intake valve opening
MBT	minimum spark advance for maximum brake torque
PFI	port fuel injection
RTD	resistance temperature detector
RTS	resistance temperature sensing
WOT	wide open throttle

## Greek symbols

$\epsilon$	compression ratio
$\lambda$	air-to-fuel equivalence ratio

## Roman Symbols

$h$	convection coefficient
$q$	heat flux
$T_g$	bulk gas temperature
$T_w$	wall temperature

## EXPERIMENTAL EQUIPMENT

The engine used in this research is a four-stroke single-cylinder spark ignited gas engine based on a CFR (Cooperative Fuel Research) engine operated at a constant speed of 600 rpm. It is equipped with PFI (port fuel injection) and a variable compression ratio. The details of the engine are given in Table 1. A cross section of the CFR-cylinder is shown in Figure 1. Fuel injection and ignition timing are controlled by a MoTeC M4Pro electronic control unit.

Table 1 CFR-Engine properties

Bore	82.55 mm
Stroke	114.2 mm
Connecting rod length	254 mm
Swept Volume	611.7 cm <sup>3</sup>
IVO	17 °CA ATDC
IVC	26 °CA ABDC
EVO	32 °CA BBDC
EVC	6 °CA ATDC

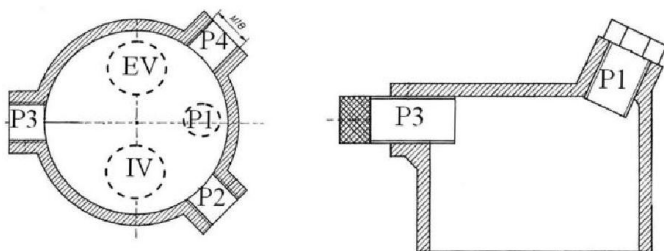


Figure 1 Cross section of the CFR engine, P1: spark plug, P2-P4: sensor positions, IV: intake valve, EV: exhaust valve

We have used a commercially available sensor to measure the heat flux and wall temperature. It is an uncoated Vatel HFM-7 sensor which consists of a thermopile (heat flux signal, HFS) and an RTD (substrate temperature signal, RTS). The sensor has a response time of 17  $\mu$ s. As the test engine is easily accessible, the heat flux sensor could be installed in three different positions (P2, P3, P4 as shown in Figure 1). These openings are placed at the same height in the cylinder wall and are equally distributed around the circumference of the cylinder. The spark plug was placed in position P1. The measurement position in this paper is always P2.

In-cylinder pressures were measured using a water-cooled Kistler 701A piezoelectric pressure sensor. Inlet pressure was measured using a Kistler 4075A20 piezoresistive pressure sensor. This inlet pressure was used to reference the in-cylinder pressure. A 12 bit data acquisition card was used to sample both the heat flux and pressure signals. It is triggered by a crank angle encoder every 0.1 °CA. This results in a sampling rate of 36 kHz. Gas flows were measured with Bronkhorst Hi-Tec F-201AC (fuel) and F-106BZ (air) flow sensors. Type K thermocouples were used to measure inlet and exhaust gas temperatures.

## RESULTS AND DISCUSSION

The compression ratio ( $\epsilon$ ), ignition timing (IGN) and air-to-fuel equivalence ratio ( $\lambda$ ) were varied for hydrogen to find the influencing parameters on engine heat transfer. All measurements on hydrogen were performed with wide-open-throttle (WOT). Measurements were done with ignition at TDC which is the MBT-timing for the stoichiometric WOT case at an  $\epsilon$  of 8.

The most common way found in the literature is to display the heat flux trace of the ensemble cycle. The heat flux of the ensemble cycle at a certain crank angle is the average of all the heat fluxes of an entire measurement set at that crank angle. In this paper heat flux traces of the ensemble cycle are shown and a measurement set always consists of 35 cycles.

An estimate of the bulk gas temperature has been made based on the equation of state and the measured in-cylinder pressure. The specific gas constant (R) and trapped mass are two unknown variables that have to be calculated. R is kept constant between IVC and EVO and is taken at initial conditions as the mass average of the specific gas constants of the air, fuel and residual gases. The composition of the residuals is for each fuel calculated out of the chemical equation of combustion. The trapped mass is the sum of the measured incoming mass (air and fuel) and the residuals. No incoming mass goes directly to the exhaust manifold because there is no valve overlap for the test engine. The residual mass is therefore determined with the equation of state at EVC using the measured cylinder pressure and assuming that the in-cylinder temperature is equal to the measured exhaust temperature.

A time-resolved convection coefficient is calculated with equation 1 (between IVC and EVO) to separate the temperature difference between the gas and the wall from other parameters which have an effect on the heat transfer. The bulk gas temperature is used as the reference temperature. The heat flux

in a combustion engine is transient, so the heat transfer process has to be assumed to be quasi-steady to define a convection coefficient with equation 1. This means that at every instant the heat flux is assumed to be proportional to the temperature difference between the gas and the wall. A so called instantaneous, spatial average convection coefficient is calculated with equation 1.

$$h = \frac{q(t)}{(T_g(t) - T_w(t))} \quad (1)$$

Where  $q(t)$  is the instantaneous heat flux,  $T_g(t)$  the instantaneous bulk gas temperature and  $T_w(t)$  is the instantaneous wall temperature.

A typical trace of the wall temperature during an engine cycle is plotted in Figure 2. The wall temperature decreases a little bit during the intake stroke because of the colder incoming mixture of air and fuel which cools the wall. The wall temperature increases with 5 to 10°C during the combustion period and decreases again near the end of the expansion and during the exhaust stroke. Figure 2 shows the influence of the increasing compression ratio on the wall temperature. The mean and the peak to peak value increase with an increasing heat flux. The wall temperature always peaks around the same moment despite the fact that the peak in the heat flux trace occurs at different times for a change in the compression ratio (see Figure 3).

All the other graphs in the paper will show the temperature difference between the gas and the wall because this is the driving factor for the heat transfer process. The influence of the compression ratio ( $\epsilon$ ), ignition timing (IGN) and mixture richness on the heat flux is investigated. All the plots will show the measured heat flux traces, the difference between the calculated gas and measured wall temperature and the calculated convection coefficient.

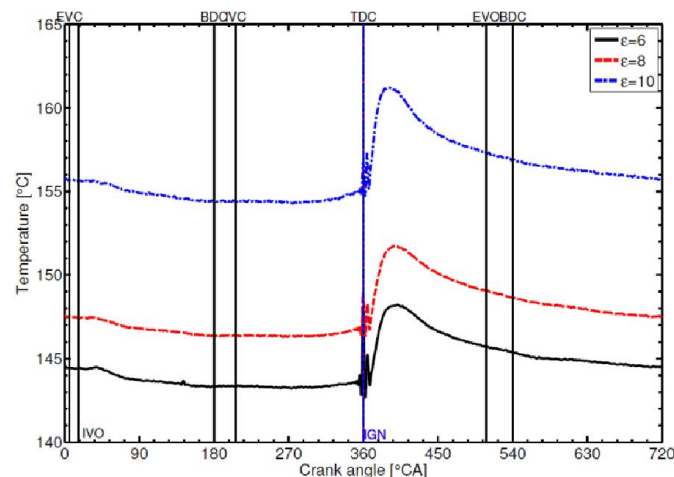


**Figure 2** The wall temperature typically has a peak to peak value of 5-10°C. The mean and peak to peak value increases with an increasing heat flux ( $\lambda=1.5$ ).

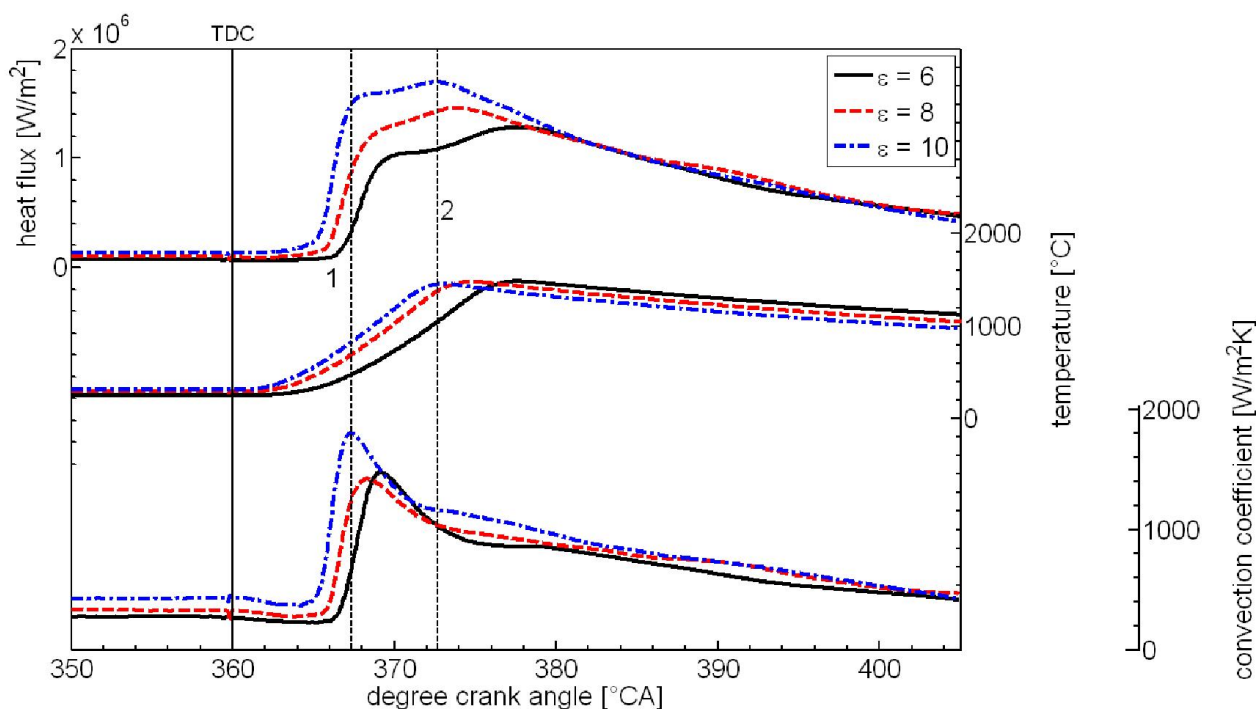


**Figure 3** Two driving forces influence the heat flux. The greatest increase in the heat flux occurs when the combustion flame passes by the measurement position (until line 1). The heat flux further increases because of the increasing difference between the gas and wall temperature (until line 2), ( $\lambda=1.5$ ).

**Compression ratio**

The compression ratio is varied from  $\epsilon=6$  to  $\epsilon=10$ . The graphs of the heat flux, the temperature difference and the convection coefficient are plotted in Figure 3. The measured heat flux increases with an increase in compression ratio. The initial rise in the heat flux trace occurs because the combustion flame passes over the measurement position. The heat flux then further increases because the temperature difference between the gas and the wall increases due to the combustion process.

A line is drawn through the maximum in the convection coefficient and temperature difference in Figure 3. Line 1 goes through the maximum of the convection coefficient and it corresponds with the end of the initial steep rise in the heat flux trace. Line 2 goes through the maximum of the temperature difference and it coincides with the maximum in the heat flux trace. This is the case for all the measurements in Figure 3. The maximum heat flux thus occurs at the moment of maximum temperature difference. But the heat transfer caused by the combustion reaches its maximum earlier when the flame has passed over the measurement position.

Although the definition of a convection coefficient is doubtful in a combustion engine, it gives more information about the heat transfer process than the measured heat flux trace alone. The effect of the temperature difference between the gas and the wall can be separated from other effects caused by the combustion process and in-cylinder movement.

According to Heywood [10] several operational properties change with increasing  $\epsilon$ : the gas pressure and peak burned gas temperature increase, gas motion increases, combustion is faster and the gas temperature late in the expansion stroke decreases. The first four properties increase the heat transfer, the last one decreases it. Figure 3 shows that the peak in the

difference between the gas temperature and the wall temperature does not increase with an increasing compression ratio (this is also the case for the gas temperature itself). However, the gas temperature is higher during the beginning of the combustion, this causes an increase in the heat flux. The black line in Figure 3 shows that the temperature difference between the gas and the wall eventually rises to the same maximum for the lowest compression ratio and this gives an extra increase in the measured heat flux (higher than expected).

There is a different trend in the maximum of the convection coefficient going from  $\epsilon=6$  to  $\epsilon=8$  compared to going from  $\epsilon=8$  to  $\epsilon=10$ . The increase in the heat flux trace from  $\epsilon=6$  to  $\epsilon=8$  is caused by an increase in the temperature difference (at the moment of flame passage). The difference between the gas and the wall temperature does not increase that strongly anymore when the compression ratio is increased from 8 to 10. Thus, the increase in the heat flux trace is more caused by the increasing gas motion and the faster combustion, this is reflected in an increase in the convection coefficient.

**Ignition timing**

The ignition timing is varied around the MBT timing to check its influence on the heat transfer, it is advanced and retarded with  $12^\circ\text{CA}$ . The measured and calculated traces are plotted in Figure 4. There is an increase in the peak of the heat flux trace with an advancing ignition timing (from 129 to 158  $\text{W}/\text{cm}^2$ ). The peak in the temperature difference between the gas and the wall increases from 1455 to 1520  $^\circ\text{C}$ . The convection coefficient increases from 1335 to 1446  $\text{W}/\text{m}^2\text{K}$ . The increase in the temperature difference and convection coefficient equally contribute to the increase in the heat flux.

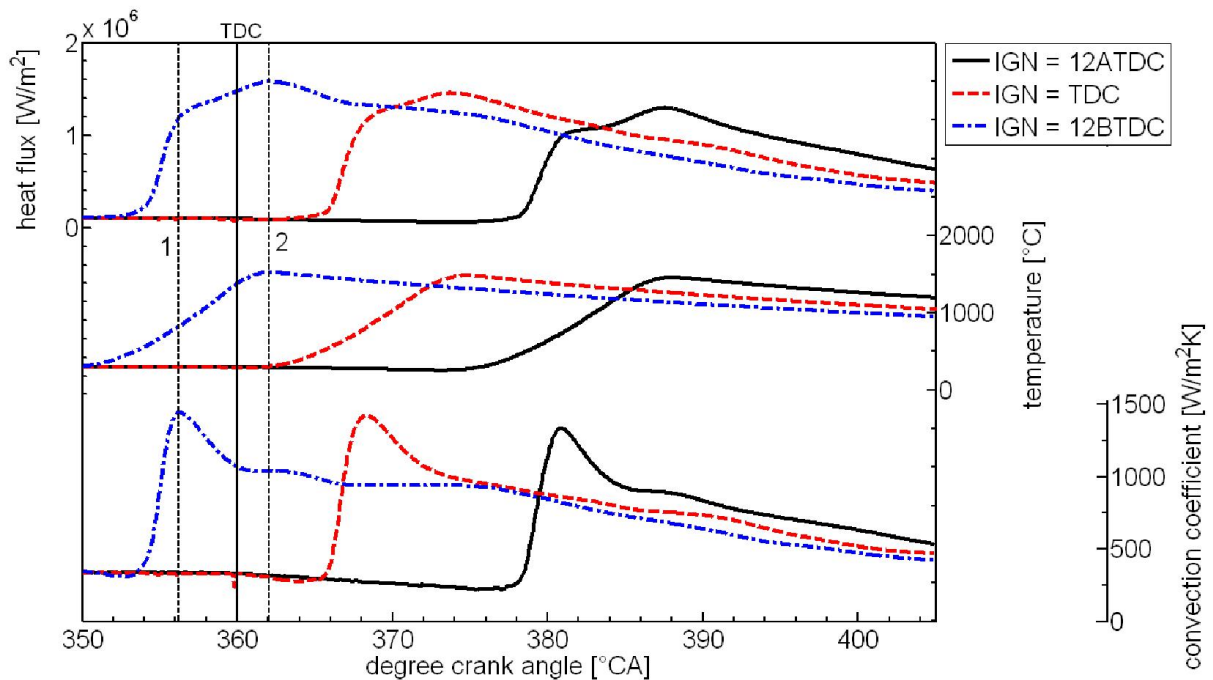


**Figure 4** The two different driving forces are again visible in the heat flux traces. The maximum heat flux occurs at the moment of the maximum temperature difference (line 2). The initial rise in the heat flux trace is caused by the combustion process, these effects are represented by the maximum in the convection coefficient (line 1), ( $\epsilon=8, \lambda=1.5$ ).

The increases in the traces are however only modest, the shift in time is the most important influence of the changing ignition timing.

The maximum in the convection coefficient corresponds again with the end of the initial rise in the heat flux trace (line 1 in Figure 4). The maximum in the heat flux occurs at the moment that the temperature difference between the wall and the gas peaks (line 2 in Figure 4). This is the case for all the measurements in Figure 4.

#### Air-to-fuel equivalence ratio

The air-to-fuel equivalence ratio ( $\lambda$ ) is varied from 1 to 2. The measured and calculated traces are plotted in Figure 5. The heat flux increases with a decreasing  $\lambda$  (increasing mixture richness).

The same trends as in the previous graphs are visible in the plotted traces. There are clearly two different groups of effects

that influence the heat transfer process. The temperature difference between the gas and the wall is the first group and its maximum corresponds with the maximum in the heat flux trace. The other effects are caused by the combustion process and in-cylinder motion, the influence of these effects is represented by the convection coefficient. Its maximum corresponds with the end of the initial rising slope in the heat flux trace. Increasing the mixture richness increases the convection coefficient. There is a larger spread in time between the maximum of the convection coefficient and the temperature difference for a lower  $\lambda$ . This causes a more stretched heat flux trace.

These measurements are all with the same ignition timing, but a leaner mixture should have an earlier ignition timing because of the slower combustion process. In future research the ignition timing will be MBT for all the measurements and not only for the basic measurement.

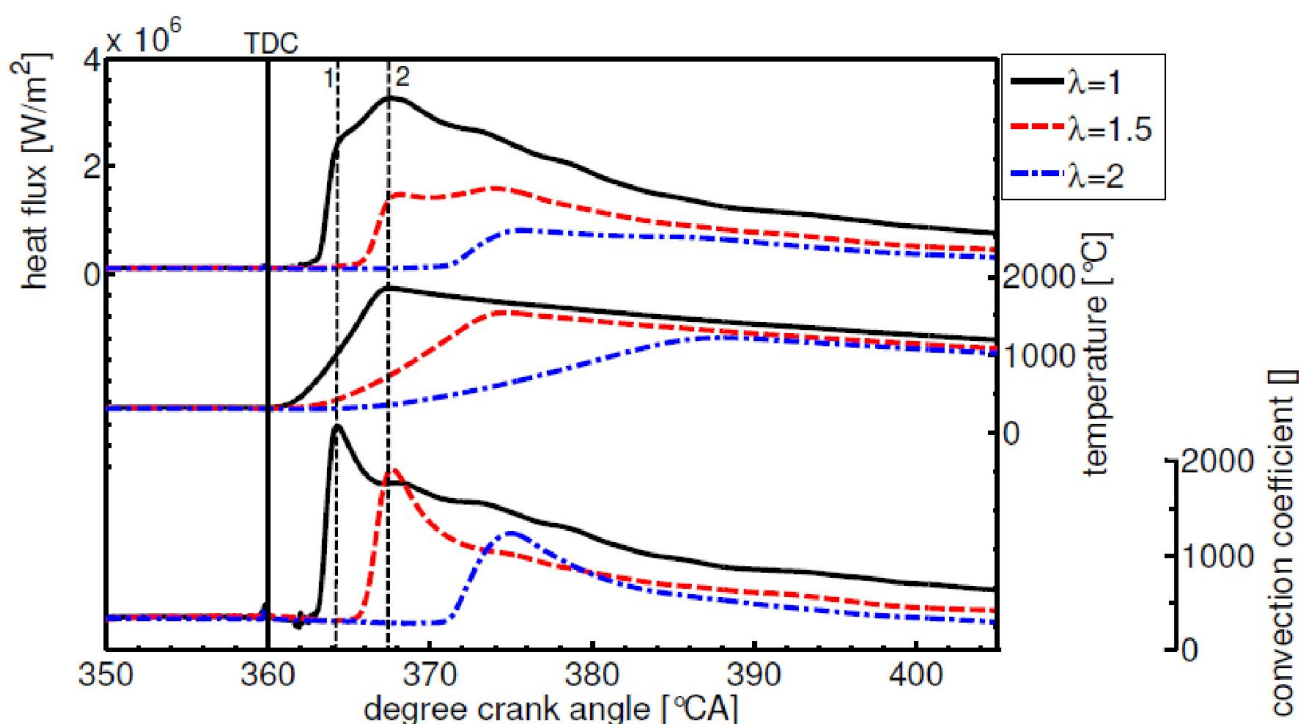


**Figure 5** The same trends are visible in the heat flux trace. The maximum heat flux occurs at the moment of the maximum temperature difference (line 2). The initial rise in the heat flux trace is caused by the combustion process, these effects are represented by the maximum in the convection coefficient (line 1), ( $\varepsilon=8$ ).

#### CONCLUSION

The heat flux and wall temperatures have been measured in a hydrogen-fuelled spark ignited combustion engine for a varying compression ratio, ignition timing and mixture richness. The effect of the temperature difference between the gas and the wall on the heat transfer, has been separated from other effects by the calculation of a convection coefficient.

This paper has demonstrated that the convection coefficient gives more insight in the heat transfer process, despite its doubtful definition in a combustion engine. It represents the influence of the combustion process and in-cylinder movement

on the heat transfer process. The maximum in the convection coefficient trace corresponded with the end of the initial rising slope of the measured heat flux for all the measurements. The maximum in the heat flux trace occurred together with the maximum in the temperature difference between the gas and the wall. The largest part of the initial increase in the heat flux is caused by the combustion process and the gas movement. The heat flux starts to rise at the moment that the combustion flame passes over the measurement position.

The heat flux increases for an increasing compression ratio. This increase is caused by an increase in the temperature difference between the gas and the wall between a compression

## 2 Topics

ratio of 6 and 8. The increase between a compression ratio of 8 and 10 is mainly caused by an increase in the gas movement and a faster combustion process.

An advanced ignition timing causes an increase in the heat flux, which is caused by a small increase in the temperature difference and the convection coefficient. The main influence of the changing ignition timing is that it shifts the traces in time.

The heat flux and convection coefficient increase with an increasing mixture richness.

### ACKNOWLEDGEMENTS

The authors of this paper would like to acknowledge the suggestions and technical assistance of Rene Janssens, Koen Chielens and Patrick De Pue. The research is funded by a Ph.D. grant (SB-81139) of the Institute for the Promotion of Innovation through Science and Technology in Flanders (IWT-Vlaanderen). This financial support is gratefully acknowledged.

### REFERENCES

1. Verhelst, S. and Wallner, T., Hydrogen-fueled internal combustion engines. *Progress in Energy and Combustion Science*, 2009. 35(6): p. 490-527.
2. Sierens, R. and Verhelst, S., Influence of the injection parameters on the efficiency and power output of a hydrogen fueled engine. *Journal of Engineering for Gas Turbines and Power-Transactions of the Asme*, 2003. 125(2): p. 444-449.
3. Verhelst, S., et al., Increasing the power output of hydrogen internal combustion engines by means of supercharging and exhaust gas recirculation. *International Journal of Hydrogen Energy*, 2009. 34(10): p. 4406-4412.
4. Verhelst, S., et al., Efficiency comparison between hydrogen and gasoline, on a bi-fuel hydrogen/gasoline engine. *International Journal of Hydrogen Energy*, 2009. 34(5): p. 2504-2510.
5. Verhelst, S. and Sierens, R., A quasi-dimensional model for the power cycle of a hydrogen-fuelled ICE. *International Journal of Hydrogen Energy*, 2007. 32(15): p. 3545-3554.
6. Verhelst, S., A Study of the Combustion in Hydrogen-Fuelled Internal Combustion Engines. Ph. D. thesis, Department of Flow, Heat and Combustion Mechanics, Ghent University - UGent, 2005.
7. Shudo, T., Nakajima, Y., and Futakuchi, T., Thermal efficiency analysis in a hydrogen premixed combustion engine. *JSAE Review*, 2000. 21(2): p. 177-182.
8. Wei, S. A Study on Transient Heat Transfer Coefficient of In-cylinder Gas in the Hydrogen Fueled Engine. in KHES and HESS, the 6th Korea-Japan Joint Symposium on Hydrogen Energy. 2001.
9. Demuynck, J., et al., Local heat flux measurements in a hydrogen and methane spark ignition engine with a thermopile sensor. *International Journal of Hydrogen Energy*, 2009. 34(24): p. 9857-9868.
10. Heywood, J.B., *Internal Combustion Engine Fundamentals*. 1988: McGraw Hill.